

CONCLUSIONS

In conclusion, within the limits discussed, the use of $\log S_c^2$ should make easier and faster the search for, and the identification of, the therapeutically best molecules. $\log S_c^2$ permits selectivity forecasting by methods and techniques analogous to the ones (quantitative structure-selectivity relationships) utilized to forecast biological activity. Moreover, $\log S_c^2$ makes it easier and faster to compare the therapeutic characteristics of different molecules since it permits selectivity quantification in the presence of many side effects.

REFERENCES

- (1) C. Hansch, A. R. Steward, and J. Iwasa, *Mol. Pharmacol.*, **1**, 87 (1965).
- (2) A. Fujinami, A. Mine, and T. Fujita, *Agr. Biol. Chem.*, **38**, 1399 (1974).
- (3) A. Fujinami, T. Satomi, A. Mine, and T. Fujita, *Pestic. Biochem. Physiol.*, **6**, 287 (1976).
- (4) W. P. Purcell, G. E. Bass, and J. Clayton, "Strategy of Drug Design: A Guide to Biological Activity," Wiley, New York, N.Y., 1973.

(5) E. Fingl and D. M. Woodbury, in "The Pharmacological Basis of Therapeutics," 4th ed., L. S. Goodman and A. Gilman, Eds., Macmillan, London, England, 1970, pp. 21, 22.

(6) G. L. Biagi, M. C. Guerra, A. M. Barbaro, and M. F. Gamba, *J. Med. Chem.*, **13**, 511 (1970).

(7) E. J. Lien, C. Hansch, and S. M. Anderson, *ibid.*, **11**, 430 (1968).

(8) E. Klarmann, V. A. Shternov, and L. W. Gates, *J. Am. Chem. Soc.*, **55**, 2576 (1933).

(9) G. L. A. Ruehle and C. M. Brewer, "United States Food and Drug Administration Methods of Testing Antiseptics and Disinfectants," Circular 198, U.S. Department of Agriculture, Dec. 1931.

(10) E. Klarmann, V. A. Shternov, and L. W. Gates, *J. Lab. Clin. Med.*, **19**, 835 (1934).

(11) G. W. Snedecor and W. G. Cochran, "Statistical Methods," 6th ed., Iowa State University Press, Ames, Iowa, 1967.

ACKNOWLEDGMENTS

The authors thank Dr. William P. Purcell, University of Tennessee, Memphis, Tenn., for helpful comments.

Hydrodynamic Characterization of a Spin-Filter Dissolution Device

J. W. MAUGER*, S. A. HOWARD, and A. KHWANGSOPHA

Received December 26, 1978, from the School of Pharmacy, West Virginia University, Morgantown, WV 26506. Accepted for publication March 1, 1979.

Abstract □ The spin-filter dissolution device was characterized using a two-dimensional convective diffusion model. Experimental model testing involved analysis of dissolution rates from nondisintegrating salicylic acid disks. The disks were prepared as double-layer tablets, with an ethylcellulose layer as a nondissolving surface. For each dissolution run, the disk was positioned so that the dissolving salicylic acid surface was parallel to the flow of the circulating fluid. Experimental variables included the stirring speed, the tablet radius, and the distance of the tablet from the stirring source. At the farthest distance from the stirring source, the average numerical exponents for stirring speed and tablet radius were 0.58 and 1.54, respectively, which compare favorably with the values of 0.50 and 1.50 from the model. When the dissolving salicylic acid surface was positioned closer to the stirring source, the numerical exponent for the stirring speed increased significantly, while the average numerical exponent for the tablet radius was lowered to 1.07, indicating a change in dissolution mechanism as a function of distance from the stirring source. These data indicate that dissolution rates are not necessarily proportional to surface area as predicted by the Nernst equation and that distance from the stirring source is significant.

Keyphrases □ Hydrodynamics—dissolution devices, spin filter, salicylic acid disks □ Models, hydrodynamic—dissolution devices, spin filter, salicylic acid disks □ Dissolution devices—spin filter, hydrodynamic analysis, models

Knowledge of critical operating variables for a dissolution device is important to the pharmaceutical scientist interested in product development, quality control, and research applications. A recent paper (1) discussed certain operating variables for the spin-filter dissolution device developed by Shah *et al.* (2). The results of this investigation indicate that the dissolution of a tablet placed in a basket is much more rapid from the face of the tablet resting on the bottom of the basket than from the face in-

side the basket. This effect was duplicated at stirring speeds of 300 and 500 rpm.

Understanding and predicting the dissolution performance for a given dissolution instrument require evaluating the instrument with a justifiable model. The purpose of the present study was to continue an evaluation of the spinning-filter device *via* a convective diffusion model based on a physically realistic and mathematically sound development.

THEORY

The model chosen is a classical one involving the flow of incompressible fluids past immersed bodies. For a nondissolving plate immersed in a fluid where the free stream velocity is U (centimeters per second), the velocity of the fluid in contact with the surface of the plate ($y = 0$) is assumed to be zero and frictional resistance retards the moving fluid in a thin layer near the wall. A property of the hydrodynamic boundary layer, h_1 (centimeters), is that its thickness is a function of the length of the plate. It is assumed that h_1 is zero at the leading edge of the plate ($x = 0$). A functional relationship between the hydrodynamic boundary layer, h_1 , the free stream velocity, U , and the length of the plate, x , is:

$$h_1 = 4.64 \left(\frac{\nu x}{U} \right)^{1/2} \quad (\text{Eq. 1})$$

Thus, h_1 increases as a function of the square root of the distance along the x axis of the plate and diminishes by a factor equal to the reciprocal square root of the free stream velocity. As Levich (3) emphasized, in reality h_1 is not a distinct distance. Instead, it represents a transition from viscous flow in the hydrodynamic boundary layer to inviscid flow in the main stream and is smooth and gradual. The thickness is commonly defined as the distance from the wall ($y = 0$) to a point where the velocity in the x direction is 90% of the free stream velocity.

A mass transfer model under conditions of forced convection can now be evaluated. Once again, visualize a plate immersed in a fluid stream.

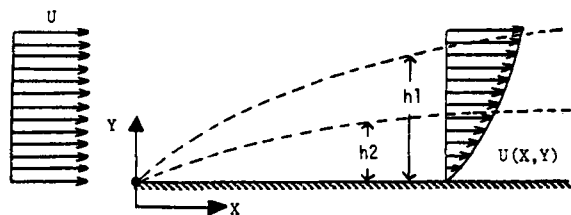


Figure 1—Development of hydrodynamic boundary layer and diffusion layer.

Now, however, the plate has a dissolving surface; as a fluid flows past the immersed solid, a hydrodynamic boundary layer, h_1 , as well as a diffusion layer, h_2 , forms (Fig. 1). The relative thickness of the two boundary layers is given by:

$$\frac{h_2}{h_1} = \left(\frac{D}{\nu}\right)^{1/3} \quad (\text{Eq. 2})$$

where D is the diffusion coefficient (square centimeters per second) of the solute and ν is the kinematic viscosity (square centimeters per second) of the dissolution fluid. For dissolving solids of pharmaceutical interest, D is $\sim 10^{-6}$ and ν for water is $\sim 10^{-2}$. Therefore, h_2/h_1 is expected to be on the order of 0.05/1. The equation that relates h_2 and h_1 is:

$$h_2 = \left(\frac{D}{\nu}\right)^{1/3} (4.46) \left(\frac{\nu x}{U}\right)^{1/2} \quad (\text{Eq. 3})$$

The diffusional flux, j (grams per second square centimeter), to the plate is:

$$j = -D \left(\frac{dc}{dy}\right) \quad (\text{Eq. 4})$$

where (dc/dy) is the concentration gradient. We are interested in evaluating (dc/dy) at the wall, *i.e.*, where $y = 0$. Differentiating a particular concentration profile¹ that provides a functional relationship between c and y yields:

$$\left(\frac{dc}{dy}\right)_{y=0} = \frac{-1.5C_s}{h_2} \quad (\text{Eq. 5})$$

Substituting the expression for h_2 from Eq. 3 gives the diffusional flux for the model shown in Fig. 1:

$$j = (0.32)(D)(C_s) \left(\frac{\nu}{D}\right)^{1/3} \left(\frac{U}{\nu x}\right)^{1/2} \quad (\text{Eq. 6})$$

where C_s is the saturation solubility (grams per cubic centimeter). This equation expresses the physical situation where the diffusional flux decreases as the reciprocal of the square root of the distance from the leading edge of the plate. As Levich (3) pointed out, different points along the plate are not uniformly accessible to diffusion. Furthermore, Eqs. 3 and 6 express a physically and mathematically defined diffusion layer rather than allow it to be empirically defined according to the commonly used Nernst equation. The mechanistic inadequacy involved with the application of the Nernst theory was commented on previously (3, 5, 6).

The governing equations for the model shown in Fig. 1 recognize velocity components and concentration gradients for both the x and y axes (3). Under particular experimental conditions, the convection term in one axis and the diffusional term in another axis may be equated with zero (5). However, the present experimental design seeks to test a model that conforms with Fig. 1.

EXPERIMENTAL

The dissolution rates were determined in a modified rotating-filter-stationary basket dissolution device^{2,3}. In place of the stationary basket, a nut and holder assembly was developed that would permit the dissolution from a constant area surface of a nondisintegrating tablet disk.

The compound selected for study was salicylic acid. Double-layer tablets of 0.624-cm radius consisted of 150 mg of salicylic acid and 150 mg of ethylcellulose; double-layer tablets of 0.451-cm radius consisted of 85 mg of salicylic acid and 85 mg of ethylcellulose. These two ingredients were compressed at 2273 kg of pressure for 15 sec on a hydraulic

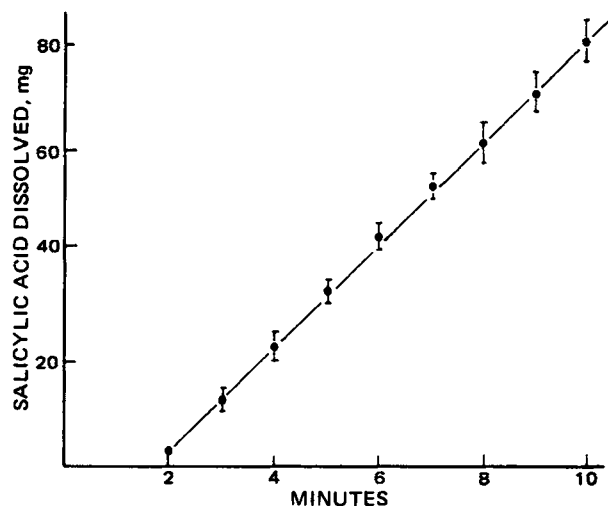


Figure 2—Typical dissolution profile for the double-layer tablet: (tablet radius of 0.624 cm, position of 1.25 cm from the stirring source, and stirring speed of 400 rpm).

press⁴. All tablets were 0.194 cm thick. Epoxy glue was used to connect the nut and double-layer tablet for use with the holder device.

The stirring speeds were controlled by a magnetic stirrer³ with a tachometer, and a strobe light was used to check the speeds. A 0.5- μ m stainless steel filter³ was used in the spinning-filter device. Temperature was maintained at 37°. The dissolution medium consisted of an aqueous solution buffered to pH 1.2 with hydrochloric acid buffer, maintaining the dissolved drug in the unionized form.

The position of the tablet in the dissolution apparatus is important. The dissolution apparatus was set up as originally described (2) with the spinning filter in a vertical position at the center of the dissolution flask. The vertically located spinning filter represents the y axis. The vertical location of the tablet was kept constant at the vertical midpoint of the spinning filter. The horizontal distance of the tablet from the spinning filter along the x axis was varied; 2.58 cm from the center of the tablet holder to the edge of the spinning filter was the *farthest* distance studied, and 1.25 cm from the center of the tablet holder to the edge of the rotating filter was the *nearest* distance studied. The nondissolving ethylcellulose side of the tablet was placed up in relation to the bottom of the flask, and the dissolving salicylic acid side was placed down and parallel to the flask bottom.

The assay was conducted spectrophotometrically at 305 nm. All experiments were conducted in the same dissolution flask, thereby eliminating cell to cell variation. The ethylcellulose did not contribute to dissolution and showed no observable change after dissolution.

The spectrophotometer was allowed to warm up for ~ 20 min before the experiment was begun. Three runs were conducted for each stirring speed, and these studies were conducted using four stirring speeds: 200, 300, 400, and 500 rpm. Samples were withdrawn automatically at known time intervals and assayed on a spectrophotometer⁵. A calibration curve confirmed linearity throughout the absorbance range used.

RESULTS AND DISCUSSION

Dissolution experiments were done in triplicate for each experimental condition. A representative dissolution profile for a particular set of experimental conditions is provided in Fig. 2. Each point shown is the average of three experiments, and the associated standard deviation is indicated by the vertical line. As anticipated, all dissolution data plotted in this way were linear and reproducible. The dissolution rates, R , were calculated from the data in Fig. 2 and a series of similar curves. For a circular disk wetted on one side, Eq. 6 becomes:

$$R = (1.58)(D)(C_s) \left(\frac{\nu}{D}\right)^{1/3} \left(\frac{U}{\nu}\right)^{1/2} (r)^{1.5} \quad (\text{Eq. 7})$$

where R is the dissolution rate (grams per second) and r is the disk radius (centimeters). A logarithmic transformation of this expression leads to:

$$\ln R = \ln A + \frac{1}{2} \ln U + 1.5 \ln r \quad (\text{Eq. 8})$$

¹ The concentration profile chosen was $C/C_s = 1 - 1.5(y/h_2) + 0.5(y/h_2)^3$. Details concerning the concentration profile and analysis of two-dimensional heat (mass) transfer models *via* Von Karman integral method are provided in Ref. 4.

² Courtesy of The Upjohn Co., Kalamazoo, Mich.

³ The Virtis Co., Gardiner, NY 12525.

⁴ Model K, hydraulic equipment, Fred S. Carver Inc., Summit, N.J.

⁵ Hitachi Ltd., Tokyo, Japan.

Table I—Dissolution Rates (Milligrams per Minute) for the Salicylic Acid Disks Positioned 2.58 cm from the Stirring Source

Stirring Speed, rpm	Tablet Radius, cm		Numerical Coefficient for Tablet Radius (0.624/0.451)
	0.451	0.624	
200	0.00400	0.00677	1.62
300	0.00485	0.00767	1.41
400	0.00591	0.01000	1.69
500	0.00687	0.01090	1.42
			1.54 ± 0.142

where:

$$A = (1.58)(D)^{2/3}(\nu)^{-1/6}(C_s) \quad (\text{Eq. 9})$$

Of initial interest is the relationship between the dissolution rate and the stirring speed. A graphical presentation of the data is given in Fig. 3, where the natural logarithm of the mean dissolution rate⁶ is plotted versus the natural logarithm of the stirring speed. The salicylic acid disks in this case were positioned 2.58 cm from the stirring source, the farthest distance studied. According to Eq. 7, the expected slope of these data is 0.5. For a tablet with a 0.451-cm radius, the least-squares slope is 0.61 with an associated standard error of 0.029; for a tablet having a 0.624-cm radius, the least-squares slope is 0.55 with an associated standard error of 0.050.

The average numerical coefficients relating the dissolution rate with the stirring speed are 0.58 for the experimental data and 0.50 according to theory. A deviation of 16% from the theory requires explanation. One possible reason is that the theory is not perfect in explaining the flow patterns developed by the spinning-filter device. The physical picture of the free stream flow patterns inherent in the model is a unidirectional flow, which is laminar and which will develop a well-behaved hydrodynamic boundary layer. The flow actually developed from the spinning-filter device is tangential.

Figure 4 is a plot of the natural logarithm of the mean dissolution rate versus the natural logarithm of stirring speed. These dissolution rates were generated with the salicylic acid disk positioned 1.25 cm from the stirring source, the nearest distance studied. The distance from the stirring source is of interest in an agitated vessel where it is reasonable to anticipate that the power generated by the stirrer will not be equally distributed throughout the vessel. The intensity of stirring is expected to be greater closer to the agitator. Therefore, the stirring coefficient may be a function of the distance of the dissolving disk from the stirring device, and these data test this relationship. For a tablet with a 0.451-cm radius, the least-squares slope is 0.80 with a standard error of 0.058; the least-squares slope for a tablet with a 0.624-cm radius is 0.66 with a standard error of 0.036. The stirring coefficients for both tablet radii are considerably above the anticipated value of 0.5 and validate the idea that the coefficient is a function of the stirring intensity or the distance of the disk from the agitation source.

An analysis of heat transfer with turbulent flow parallel to a flat plate

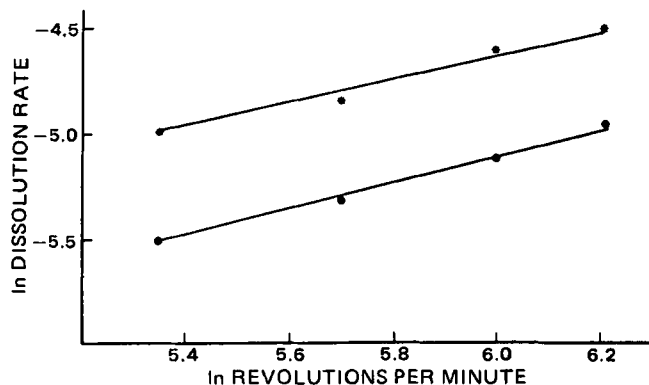


Figure 3—Natural logarithm of dissolution rate versus natural logarithm of stirring speed for salicylic acid disks positioned 2.58 cm from the stirring device. Key (tablet radius): ●, 0.451 cm; and *, 0.624 cm.

⁶ Each point in Figs. 3 and 4 represents the average slopes from the dissolution profiles similar to those shown in Fig. 2.

Table II—Dissolution Rates (Milligrams per Minute) for the Salicylic Acid Disks Positioned 1.25 cm from the Stirring Source

Stirring Speed, rpm	Tablet Radius, cm		Numerical Coefficient for Tablet Radius (0.624/0.451)
	0.451	0.624	
200	0.00406	0.00640	1.40
300	0.00638	0.00860	0.920
400	0.00734	0.00980	0.890
500	0.00846	0.01190	1.05
			1.07 ± 0.234

(7) leads to a coefficient of 0.6–0.8. Therefore, the experimental stirring coefficients at closer distances may imply that a turbulent hydrodynamic boundary is present, with the result that the dissolution rate is more sensitive to the stirring speed. This finding is of practical importance because it indicates that one must be sensitive to the distance variable to generate reproducible dissolution data.

Further analysis shows that the average numerical coefficient relating the functional dependence of the dissolution rate with the tablet radius for a tablet positioned farthest from the stirring source is 1.54 (Table I). The expected value for the model is 1.5, and verification of this numerical coefficient is particularly important with regard to understanding the dissolution mechanism. As already discussed, the model expresses the fact that the dissolving plate is not uniformly accessible to diffusion.

This concept is inherent in the mathematical expressions given by Eqs. 3, 5, and 6 for the diffusion layer thickness. It is also important to compare this relationship with the commonly used Nernst theory, where one would expect the dissolution rate to be related to area and the expected numerical coefficient is 2 (area = πr^2). As Nelson and Shah (5, 6) verified, the Nernst theory does not provide for mechanistic insight under certain conditions of forced convection.

The data in Table II are for a tablet positioned closest to the stirring device and show that the average numerical coefficient for the tablet radius is 1.07, which is considerably lower than the expected value for the model of 1.5. More importantly, the coefficient varies with stirring speed. At 200 rpm, the coefficient is 1.40 and decreases noticeably at stirring speeds of 300, 400, and 500 rpm. Therefore, the original model is not successful in predicting the functional relationship between the dissolution rate and the tablet radius. The apparent lack of parallelism between the two curves shown in Fig. 4 leads one to believe that the original model must be modified to include an interaction term between the stirring speed and the tablet radius⁷ to account for the apparent difference in flow patterns across the entire dissolution surface.

To learn more about the flow patterns, visualization studies were accomplished by adding phenolphthalein to the salicylic acid portion of the disk. The colored indicator appeared when the salicylic acid disk dissolved in an aqueous medium alkalized with sodium hydroxide, thus allowing the flow pattern to be seen. In particular, patterns across the surface of the dissolving disk could be seen in detail. Colored photographs

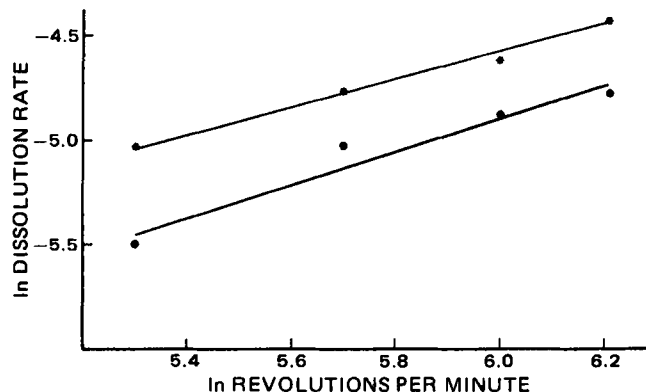


Figure 4—Natural logarithm of dissolution rate versus natural logarithm of stirring speed for salicylic acid disks positioned 1.25 cm from the stirring device. Key (tablet radius): ●, 0.451 cm; and *, 0.624 cm.

⁷ From statistical analysis of the data, there is insufficient evidence to indicate that the two lines are not parallel at the 0.05 level of significance, but a lack of parallelism exists at the 0.10 level of significance.

were taken at the near and far positions with the filter turning at 300 rpm. These photographs showed that the flow at the tablet surface was uniform and parallel to the filter face with an even color distribution when the disk was at the far position from the stirring source. The tailing streams of color away from the tablet revealed the tangential nature of the stirring patterns. This overall visualization is reasonably close to that assumed by the model and is in keeping with the data analysis from the dissolution experiments.

For the near position, the colored photographs showed that the flow pattern at the surface was less uniform and in the direction of the spinning filter rather than parallel to it. Furthermore, a concentration of color appeared on the filter side of the tablet. The visualization procedure combined with dissolution data confirms that the flow pattern is influenced by the distance from the rotating stirring source. Dissolution rates measured from disintegrating tablets would presumably be influenced in a similar way, making basket placement a critical factor.

SUMMARY

At the farthest distance from the stirring source, the average numerical exponents for stirring speed and tablet radius were 0.58 and 1.54, respectively, which compares favorably with the theoretical values of 0.50 and 1.50. When the dissolving salicylic acid surface was positioned closer to the stirring source, the numerical exponent for the tablet radius was

lowered to 1.07, indicating a change in dissolution as a function of distance from the stirring source. These data indicate that dissolution rates are not necessarily proportional to surface area, as predicted by the Nernst equation, and that distance from the stirring source is a significant factor. Convective diffusion models combined with easily accomplished visualization techniques provide the methodology needed to characterize various dissolution devices.

REFERENCES

- (1) S. Howard, J. Mauger, A. Khwangsopha, and D. Pasquarelli, "Operating Variables for the Spin Filter Dissolution Device," presented at APhA Academy of Pharmaceutical Sciences, New York meeting, May 1977.
- (2) A. C. Shah, C. B. Peot, and J. F. Ochs, *J. Pharm. Sci.*, **62**, 671 (1973).
- (3) V. Levich, "Physicochemical Hydrodynamics," Prentice Hall, Englewood Cliffs, N.J., 1962.
- (4) J. Knudsen and D. Katz, "Fluid Dynamics and Heat Transfer," McGraw-Hill, New York, N.Y., 1958, pp. 247-259, 473-481.
- (5) K. G. Nelson and A. C. Shah, *J. Pharm. Sci.*, **64**, 610 (1975).
- (6) A. C. Shah and K. G. Nelson, *ibid.*, **64**, 1519 (1975).
- (7) J. Kestin and L. N. Persen, *Int. J. Heat Mass Transfer*, **5**, 355 (1962).

Linear Pharmacokinetics of Orally Administered Fenopropfen Calcium

J. F. NASH^x, L. D. BECHTOL, C. A. BUNDE^{*}, R. J. BOPP, K. Z. FARID, and C. T. SPRADLIN

Received October 6, 1978, from the Lilly Research Laboratories, Indianapolis, IN 46206.

Accepted for publication February 20, 1979.

^{*}Present address: Cintest, Inc., Cincinnati, OH 45220.

Abstract □ The bioavailability of fenopropfen from three different fenopropfen calcium capsule formulations containing the equivalent of 60, 165, and 300 mg of fenopropfen was determined in two studies. In the first study, 12 subjects received one capsule of each formulation according to a three-period crossover design. The second study required each of 13 subjects to receive 300 mg of fenopropfen equivalent of the 60- and 300-mg capsules and 330 mg of the 165-mg capsule. The initial study provided information on the linearity of fenopropfen pharmacokinetics, and the second study established that the three capsule formulations were bioequivalent. The bioavailability parameters C_{max} , t_{max} , and $AUC_{0-12 hr}$ for the drug in plasma were consistent with a linear pharmacokinetic model, as were the amounts of fenopropfen and hydroxyfenopropfen excreted in the urine. These data show linearity of kinetics for fenopropfen in plasma throughout the 60-300-mg dosage range after a single dose. Physical measurements of each capsule formulation drug content, weight variation, and dissolution showed the products to be uniform and readily soluble.

Keyphrases □ Fenopropfen—pharmacokinetics, oral administration, calcium salt □ Pharmacokinetics—fenopropfen calcium, oral administration □ Anti-inflammatory agents—fenopropfen calcium, pharmacokinetics, oral administration

Fenopropfen calcium¹ was shown to be a useful anti-inflammatory agent in osteoarthritis (1-4) and rheumatoid arthritis (5-16) in adults. To extend the therapeutic range of the compound, drug formulations containing 60-300 mg of fenopropfen equivalent as fenopropfen calcium² were selected for juvenile rheumatoid arthritis studies. This paper

reports the linearity of fenopropfen pharmacokinetics, fenopropfen bioavailability, and the uniformity of drug excretion after a single-dose oral administration of capsules containing 60, 165, or 300 mg of fenopropfen equivalent in an adult population.

EXPERIMENTAL

Clinical Study Protocol—Healthy adult male volunteers, 18-50 years old, participated in the two studies. Their weight was $\pm 10\%$ of the ideal weight (17). The subjects had no history of significant GI disorder; hepatic, renal, hematological, or cardiovascular disease; or chronic alcoholism. Each subject underwent a urinalysis, hematology, and blood analysis³ as well as a physical examination to ensure inclusion of only subjects in good health.

In the first bioavailability study, 12 subjects were placed into Groups I, II, and III. Each group consisted of four subjects, each of whom received a single capsule of 60, 165, or 300 mg of fenopropfen equivalent (Table I) on three consecutive occasions, with a 2-day washout period between each dose. Each subject was instructed to adhere to a standard protocol and

Table I—Fenopropfen Calcium Capsule Formulas^a

Ingredient	Capsule ^b , mg		
	60	165	300
Fenopropfen calcium	70.0	192.5	350.0
Silicone fluid 350 centistokes	3.0	8.2	15.0
Microcrystalline cellulose with carboxymethylcellulose sodium ^c	217.0	179.2	125.0

^a Values in milligrams. ^b Fenopropfen equivalent. ^c Avicel RC-591 MCC, FMC Corp.

³ SMA 12/60.

¹ Nalfon, Dista Products Co. (a Division of Eli Lilly and Co.).

² Drug weight is reported in this paper as fenopropfen equivalent of fenopropfen calcium.